

Navigating Robot Swarm Through a Virtual Tube with Flow-Adaptive Distribution Control

Yongwei Zhang, Shuli Lv, Kairong Liu, Quanyi Liang, Quan Quan, *Senior Member, IEEE*, and Zhikun She

Abstract—With the rapid development of robot swarm technology and its diverse applications, navigating robot swarms through complex environments has emerged as a critical research direction. To ensure safe navigation and avoid potential collisions with obstacles, the concept of virtual tubes has been introduced to define safe and navigable regions. However, current control methods in virtual tubes face the congestion issues, particularly in narrow virtual tubes with low throughput. To address these challenges, we first originally introduce the concepts of virtual tube area and flow capacity, and develop an new evolution model for the spatial density function. Next, we propose a novel control method that combines a modified artificial potential field (APF) for swarm navigation and density feedback control for distribution regulation, under which a saturated velocity command is designed. Then, we generate a global velocity field that not only ensures collision-free navigation through the virtual tube, but also achieves locally input-to-state stability (LISS) for density tracking errors, both of which are rigorously proven. Finally, numerical simulations and realistic applications validate the effectiveness and advantages of the proposed method in managing robot swarms within narrow virtual tubes.

Index Terms—robot swarm, virtual tube, safe navigation, distribution regulation, density feedback control.

I. INTRODUCTION

Navigating robot swarms through complex environments is a crucial challenge for broad applications, including environmental monitoring, drug delivery, and disaster response [1]–[4]. In environments with dense obstacles, the concepts of general and optimal virtual tubes have been developed [5], [6]. These virtual tubes create safe and obstacle-free zones, making the navigation of robot swarms through these predefined regions the main consideration. Recent works have proposed control methods for safe navigation within virtual tubes [7], [8]. However, navigating robot swarms safely through narrow virtual tubes with low throughput poses challenges, such as congestion and collisions. To address these issues, this article proposes a control framework that incorporates swarm distribution regulation into safe navigation, ensuring collision-free and efficient traversal.

The primary challenge in navigating robot swarms safely through virtual tubes involves two aspects: enabling the robots

to adapt to the tube’s throughput and preventing collisions with the tube boundaries and with each other. Existing control strategies can be broadly classified into two categories: bottom-up and top-down [9]. Bottom-up approaches, such as formation control [10] and distributed multi-agent trajectory planning [11], are effective for small-scale swarms. However, as the swarm size grows, these approaches often suffer from reduced feasibility and stability, making them increasingly challenging to implement. For swarm navigation, control-based methods are more commonly employed, including artificial potential fields (APF) [12], vector fields [13], control barrier functions (CBF) [14], and flocking techniques [15]. These approaches are advantageous for their low computational and communication requirements, as well as their ability to adapt quickly to dynamic environments, making them particularly well-suited for multi-robot systems. However, when navigating through narrow passages, they may fail to ensure both safety and efficiency [16].

In recent years, top-down approaches have gained significant attention for their ability to model the macroscopic behaviors of robot swarms using evolutionary frameworks. The continuous-time Markov chain method is one of the notable approaches, which partitions the workspace into multiple sub-regions, assigns probability density distributions to these regions, and designs transition rates to achieve a desired distribution [17]. However, this method has a key limitation: it neglects the underlying dynamics of individual robots. The mean-field method is another prominent top-down approach, which leverages the Fokker–Planck equation to model the evolution of mean-field density. By incorporating robot dynamics with stochastic effects, this method enables the design of a global velocity field to guide swarms toward specified configurations [18], [19]. For large-scale swarms with deterministic dynamics, the continuity equation in fluid mechanics is used to describe the evolution of robot density [20], [21]. However, the density evolution models in [18]–[21] treat robots as particles, ignoring their actual safety size and neglecting collision avoidance between robots. Therefore, applying these approaches for robots in narrow spaces involves substantial difficulties.

The control strategy proposed in this article integrates a modified artificial potential field (APF) with density feedback control techniques. For motion control of robots within the virtual tube, a line-integral Lyapunov function and two Lyapunov-like barrier functions in [22] are introduced to ensure collision-free navigation. To regulate swarm distribution, a density evolution model is developed, linking the dynamics of individual robots to their collective behavior. Leveraging density feedback, a global velocity field is designed to guide

Yongwei Zhang, Kairong Liu, Quanyi Liang and Zhikun She are with the School of Mathematical Sciences, Beihang University, Beijing 100191, China (e-mail: zhangyongwei@buaa.edu.cn; krlu@buaa.edu.cn; qyliang@buaa.edu.cn; zhikun.she@buaa.edu.cn).

Shuli Lv and Quan Quan are with the School of Automation Science and Electrical Engineering, Beihang University, Beijing 100191, China (e-mail: lvshuli@buaa.edu.cn; qq_buaa@buaa.edu.cn).

Corresponding authors: Quan Quan and Zhikun She.

This work was supported by the National Key Research and Development Program of China (No. 2022YFA1005103), National Natural Science Foundation of China (NSFC 12371452, NSFC 12401574).

the swarm toward the desired spatial distribution, dynamically adjusted according to the tube's throughput.

The traversal scheme proposed in [22] is effective for general virtual tubes but becomes less suitable in narrow ones, where it can lead to excessively dense distributions and heightened safety risks. Similarly, control laws introduced in [18]–[21] focus on the distribution control of large-scale robot swarms but neglect the safety area of individual robots, increasing the likelihood of collisions when directly implemented. In contrast, this work specifically addresses the challenges of traversal in narrow virtual tubes by proposing a distribution-regulating control framework, which enables safe and efficient swarm navigation while ensuring stability in tracking the desired density distribution. The main contributions of this article are as follows:

- **Extension of virtual tube model and density evolution model:** The concepts of virtual tube area and flow capacity are originally introduced, and a density evolution model for robot swarms is newly developed. These concepts facilitate effective control of swarm distribution, particularly in narrow virtual tubes.
- **Integration of microscopic and macroscopic dynamics:** Both robot collision avoidance (microscopic dynamics) and swarm density evolution (macroscopic dynamics) are considered. It enables the macroscopic configuration control of robot swarms within virtual tubes, while ensuring no collisions occur between robots.
- **Design of a simple and saturated velocity command:** By integrating a modified artificial potential field (APF) with density feedback control techniques, a novel and saturated velocity command composed of simple terms is designed. This command effectively reduces congestion during traversal through narrow virtual tubes.
- **Guarantee of safety and stability of the proposed method:** A global velocity field corresponding to the proposed velocity command is generated, under which the robot swarm's safe navigation within the virtual tube and locally input-to-state stability (LISS) of the density tracking errors is rigorously proven.

II. PRELIMINARIES

In this section, we first introduce the notation used in this article. Next, we present a general virtual tube model, upon which we newly introduce the concepts of virtual tube area and flow capacity, which are essential for swarm distribution control. Then, we provide a typical robot kinematic model and assume the velocity is saturated. Finally, we define the spatial density function of the robot swarm and innovatively develop its evolution model within the virtual tube.

A. Notation

Let $E \subset \mathbb{R}^2$ be a measurable set and $T > 0$ be a constant. Set $E_T = E \times (0, T]$. Denote $L^2(E) = \{f : \|f\|_{L^2(E)} := (\int_E |f(x)|^2 dx)^{1/2} < \infty\}$, endowed with the norm $\|\cdot\|_{L^2(E)}$. Denote $L^\infty(E) = \{f : \|f\|_{L^\infty(E)} := \text{ess sup}_{x \in E} |f(x)| < \infty\}$, endowed with the norm $\|\cdot\|_{L^\infty(E)}$. Denote $L^\infty(E_T) = \{f : \|f\|_{L^\infty(E_T)} := \text{ess sup}_{(x,t) \in E_T} |f(x,t)| < \infty\}$, endowed

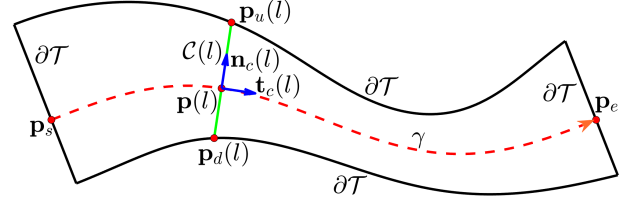


Fig. 1. The general virtual tube model.

with the norm $\|\cdot\|_{L^\infty(E_T)}$. $\|\cdot\|$ is the 2-norm of a vector. $|\cdot|$ is the absolute value of a scalar. The inner product operator is denoted as \cdot . Let \mathcal{T} be a bounded and connected domain (thus measurable) in \mathbb{R}^2 and $\partial\mathcal{T}$ be its boundary. Set $\mathcal{T}_T = \mathcal{T} \times (0, T]$ and $S(\mathcal{T}_T) = \partial\mathcal{T} \times [0, T]$. For a function $f(\mathbf{x}, t) : \mathcal{T}_T \rightarrow \mathbb{R}$, \mathbf{x} is the spatial variable and t is the time variable. Let x_i be the i th coordinate of \mathbf{x} , denote $\partial_i f = \frac{\partial f}{\partial x_i}$. ∇ is the gradient operator acting on scalar functions, and $\nabla \cdot$ is the divergence operator acting on vector fields. The two operators are only taken with respect to the spatial variable \mathbf{x} . (x, y) and $\langle l, r \rangle$ are the coordinate representations in the Cartesian and curvilinear coordinate systems, respectively.

B. General Virtual Tube Model

In this subsection, we introduce the general virtual tube model in \mathbb{R}^2 , which consists of two parts: generating curve and cross-section [22].

1) **Generating Curve.** Given a differentiable generating curve $\gamma(l)$, starting at \mathbf{p}_s and ending at \mathbf{p}_e , where $l \in [0, L]$ is the arc length parameter. As shown in Figure 1, there exists $\mathbf{p} \in \gamma$ with arc length parameter l , $\mathbf{t}_c(l) := \frac{\dot{\gamma}(l)}{|\dot{\gamma}(l)|}$ is the unit tangent vector, and $\mathbf{n}_c(l) := \left(-\frac{\dot{\gamma}_2(l)}{|\dot{\gamma}(l)|}, \frac{\dot{\gamma}_1(l)}{|\dot{\gamma}(l)|}\right)$ is the unit normal vector in the counterclockwise direction [5], [23].

2) **Cross-section.** The cross-section passing $\mathbf{p}(l)$ is defined as $\mathcal{C}(l) = \{\mathbf{x} \in \mathbb{R}^2 : \mathbf{x} = \mathbf{p}(l) + \lambda(l)\mathbf{n}_c(l), -r_d(l) \leq \lambda(l) \leq r_u(l), r_d(l), r_u(l) > 0\}$. Obviously, two endpoints $\mathbf{p}_d(l), \mathbf{p}_u(l) \in \mathcal{C}(l)$ are $\mathbf{p}_d(l) = \mathbf{p}(l) - r_d(l)\mathbf{n}_c(l)$ and $\mathbf{p}_u(l) = \mathbf{p}(l) + r_u(l)\mathbf{n}_c(l)$, respectively. With $\gamma(l)$ and $\mathcal{C}(l)$, a general virtual tube is defined as

$$\mathcal{T} = \cup_{l \in [0, L]} \mathcal{C}(l). \quad (1)$$

Then the boundary of \mathcal{T} is formulated as $\partial\mathcal{T} = \mathcal{C}(0) \cup \mathcal{C}(L) \cup \{\mathbf{p}_d(l) : l \in [0, L]\} \cup \{\mathbf{p}_u(l) : l \in [0, L]\}$. Let the boundary excluding two terminal cross-sections $\mathcal{C}(0)$ and $\mathcal{C}(L)$ be $\partial\mathcal{T}' = \partial\mathcal{T} \setminus \{\mathcal{C}(0) \cup \mathcal{C}(L)\}$.

Meanwhile, the following assumption is required to ensure that any two distinct cross-sections within the virtual tube \mathcal{T} do not intersect.

Assumption 1: For any $l_1, l_2 \in [0, L]$, $l_1 \neq l_2$, $\mathcal{C}(l_1) \cap \mathcal{C}(l_2) = \emptyset$.

Then, we define the virtual tube that satisfies Assumption 1 as a *regular* virtual tube. In contrast, if two cross-sections intersect, the virtual tube is referred to as an *irregular* virtual tube. As shown in Figure 2, the regular virtual tube contains no intersecting cross-sections, whereas the two terminal cross-sections of the irregular virtual tube intersect at one single point.

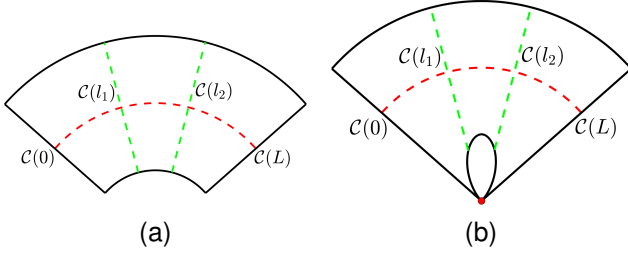


Fig. 2. (a) Regular virtual tube. (b) Irregular virtual tube.

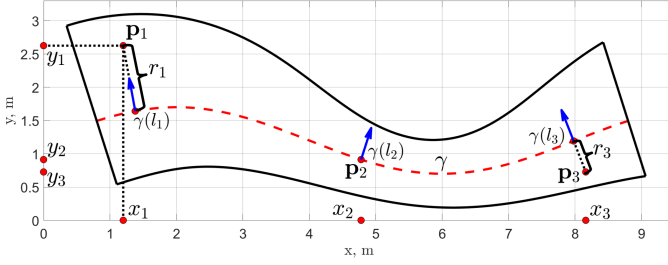


Fig. 3. Cartesian and curvilinear coordinate representations of three points.

In the following, we refer to \mathcal{T} as the regular virtual tube. Therefore, for any point $\mathbf{p} = (x_{\mathbf{p}}, y_{\mathbf{p}}) \in \mathcal{T}$ in the Cartesian coordinate system, there exists a unique arc length parameter $l_{\mathbf{p}}$ and the corresponding cross-section $\mathcal{C}(l_{\mathbf{p}})$ that contains \mathbf{p} . Let $r_{\mathbf{p}} := \|\mathbf{p} - \gamma(l_{\mathbf{p}})\|$ represent the distance between \mathbf{p} and $\gamma(l_{\mathbf{p}})$. In the curvilinear coordinate system, the coordinates of \mathbf{p} are given by $\langle l_{\mathbf{p}}, r_{\mathbf{p}} \rangle$ if $(\mathbf{p} - \gamma(l_{\mathbf{p}})) \cdot \mathbf{n}_c(l_{\mathbf{p}}) \geq 0$; otherwise, the coordinates are $\langle l_{\mathbf{p}}, -r_{\mathbf{p}} \rangle$. As shown in Figure 3, in the Cartesian coordinate system, the coordinates of the points \mathbf{p}_1 , \mathbf{p}_2 , and \mathbf{p}_3 are (x_1, y_1) , (x_2, y_2) , and (x_3, y_3) , respectively. In the curvilinear coordinate system, their corresponding coordinates are $\langle l_1, r_1 \rangle$, $\langle l_2, 0 \rangle$, and $\langle l_3, -r_3 \rangle$, respectively. The coordinates $\langle l, r \rangle$ are explained as follows: starting from \mathbf{p}_s , move a distance l along the generating curve γ to $\gamma(l)$, then move a distance r (or $-r$) along the normal direction $\mathbf{n}_c(l)$ (or $-\mathbf{n}_c(l)$) to reach the corresponding point.

For $\mathbf{p} \in \mathcal{T}$ with Cartesian coordinates $(x_{\mathbf{p}}, y_{\mathbf{p}})$ and curve coordinates $\langle l_{\mathbf{p}}, r_{\mathbf{p}} \rangle$, let Ψ be the coordinate transformation, let π_1 be the projection operator. Assumption 1 ensures that Ψ is a one-to-one correspondence. Then, the relationship between $(x_{\mathbf{p}}, y_{\mathbf{p}})$ and $l_{\mathbf{p}}$ can be expressed by the following mapping:

$$\begin{aligned} \omega : \mathcal{T} &\xrightarrow{\Psi} \mathcal{T} \xrightarrow{\pi_1} \mathbb{R}, \\ (x_{\mathbf{p}}, y_{\mathbf{p}}) &\mapsto \langle l_{\mathbf{p}}, r_{\mathbf{p}} \rangle \mapsto l_{\mathbf{p}}, \\ \omega((x_{\mathbf{p}}, y_{\mathbf{p}})) &= \pi_1(\Psi(x_{\mathbf{p}}, y_{\mathbf{p}})) = \pi_1(\langle l_{\mathbf{p}}, r_{\mathbf{p}} \rangle) = l_{\mathbf{p}}. \end{aligned} \quad (2)$$

C. Definition of Virtual Tube Area and Flow Capacity

Based on the general virtual tube model, in this subsection, we define the virtual tube area and flow capacity, which are used for the design and control of the robot swarm's macroscopic configuration in the subsequent sections. To start with, the following assumption is necessary.

Assumption 2: For $l \in [0, L]$, suppose that $r_d(l)$ and $r_u(l)$ are continuous and differentiable.

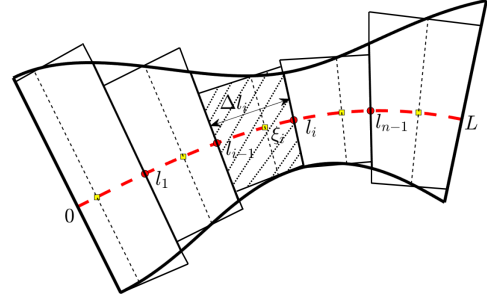


Fig. 4. Schematic diagram for the definition of virtual tube area.

After that, similar to the definition of the definite integral for a single-variable function, we define the virtual tube area using the approach of partitioning, approximating sums, and taking limits.

1) **Partitioning.** In the virtual tube shown in Figure 4, let $n - 1$ points be arbitrarily selected on the generating curve γ , with their arc length parameters successively being $0 = l_0 < l_1 < \dots < l_{n-1} < l_n = L$. These points partition γ into n small curve segments, with the corresponding arc length parameter intervals being $[l_{i-1}, l_i]$. Let $\Delta l_i := l_i - l_{i-1}$ and $\Delta := \max_{1 \leq i \leq n} \{\Delta l_i\}$.

2) **Approximating Sums.** Assuming that the partition points are sufficiently numerous and the partition is sufficiently fine, the curve segment between $\gamma(l_{i-1})$ and $\gamma(l_i)$ can be approximated as a straight line segment of length Δl_i . For each small interval $[l_{i-1}, l_i]$, let us arbitrarily choose an arc length parameter $\xi_i \in [l_{i-1}, l_i]$, then construct a small rectangle with a base of Δl_i and a height of $r_d(\xi_i) + r_u(\xi_i)$. Under Assumption 2, both r_d and r_u are continuous, hence their values on $[l_{i-1}, l_i]$ are nearly identical. Consequently, the area of the virtual tube can be approximated by the Riemann sum $S_n = \sum_{i=1}^n (r_d(\xi_i) + r_u(\xi_i)) \Delta l_i$.

3) **Taking Limits.** Due to the continuity of r_d and r_u on the closed interval $[0, L]$, for arbitrarily chosen set $\{\xi_i\}$, as $\Delta \rightarrow 0$, there exists $S_n \rightarrow S$, where S is a definite real number.

Definition 1: Define S as the area of the virtual tube, denoted by $S = \int_0^L (r_d(l) + r_u(l)) dl$.

Subsequently, let $r_c(l) := \frac{r_d(l) + r_u(l)}{2}$ be the radius of the cross-section $\mathcal{C}(l)$, and denote $\Delta S = \int_0^{l+\Delta l} 2r_c(s) ds - \int_0^l 2r_c(s) ds$. Near the cross-section $\mathcal{C}(l)$, the rate of change in the area of the virtual tube can be expressed as: $\lim_{\Delta l \rightarrow 0} \frac{\Delta S}{\Delta l} = \lim_{\Delta l \rightarrow 0} \frac{\int_l^{l+\Delta l} 2r_c(s) ds}{\Delta l} = \frac{2r_c(l)\Delta l}{\Delta l} = 2r_c(l)$, where the penultimate equality utilizes the continuity of $r_c(l)$. This rate is directly proportional to the radius of the cross-section $\mathcal{C}(l)$. For simplicity, we neglect the coefficient and provide the following definition of flow capacity.

Definition 2: Define $\sigma(l) := r_c(l)$ as the flow capacity of the cross-section $\mathcal{C}(l)$.

From Definition 2, a larger $\sigma(l)$ implies that the cross-section $\mathcal{C}(l)$ can accommodate more robots. With $\sigma(l)$, we can finally define $\mathcal{C}(l)$ as a narrow cross-section if $r_s < \sigma(l) \leq 2r_s$, where r_s is the safety radius of a robot [22]. In this case, the narrow cross-section can accommodate a maximum of one robot. Specifically, if \mathcal{T} contains a narrow cross-section, then

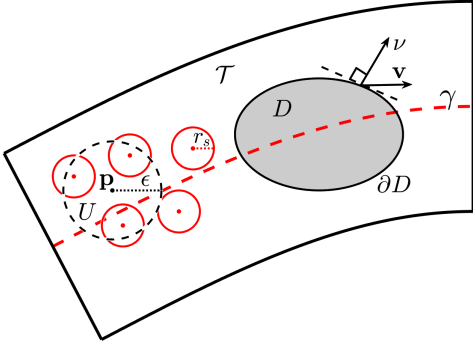


Fig. 5. Schematic diagram for the approximation of the density of robots and the density evolution model.

it is defined as the narrow virtual tube.

D. Single Robot Kinematic Model

In this subsection, we present the typical kinematic model of a single robot. The robot swarm consists of N robots, all robots are assumed homogeneous and modeled as

$$d\mathbf{p}_i = \mathbf{v}_i dt, \quad i = 1, \dots, N \quad (3)$$

where $\mathbf{p}_i \in \mathbb{R}^2$ is the position of the i th robot, $\mathbf{v}_i := \mathbf{v}(\mathbf{p}_i, t) \in \mathbb{R}^2$ is the velocity, with \mathbf{v}_i obtained by the global vector field \mathbf{v} acting on \mathbf{p}_i .

Besides, \mathbf{v}_i is subject to energy constraints with a maximum speed v_{\max} . Thus, \mathbf{v}_i is saturated as

$$\mathbf{v}_i = \text{sat}(\mathbf{u}_i, v_{\max}) = \kappa_m(\mathbf{u}_i)(\mathbf{u}_i), \quad (4)$$

where \mathbf{u}_i is the unsaturated velocity and

$$\text{sat}(\mathbf{u}_i, v_{\max}) := \begin{cases} \mathbf{u}_i, & \|\mathbf{u}_i\| \leq v_{\max} \\ v_{\max} \frac{\mathbf{u}_i}{\|\mathbf{u}_i\|}, & \|\mathbf{u}_i\| > v_{\max} \end{cases},$$

$$\kappa_m(\mathbf{u}_i) := \begin{cases} 1, & \|\mathbf{u}_i\| \leq v_{\max} \\ \frac{v_{\max}}{\|\mathbf{u}_i\|}, & \|\mathbf{u}_i\| > v_{\max} \end{cases}.$$

Obviously, $0 < \kappa_m(\mathbf{u}_i) \leq 1$, henceforth it will be denoted as κ_m for brevity.

E. Robot Swarm Evolution Model

In this subsection, we develop our new evolution model for a robot swarm within the virtual tube. The modeling approach is inspired by the *continuity equation* [24] in fluid mechanics.

Firstly, as shown in Figure 5, consider a position $\mathbf{p} \in \mathcal{T}$ at time $t \in [0, T]$. Similar to the definition of mass density in fluids, we introduce the concept of *local averaging* to estimate the robot density at position \mathbf{p} . To do this, the neighborhood of \mathbf{p} must be first determined. Let $\epsilon_{\min} > 0$ be a constant (see Remark 1 below for a detailed explanation), and denote $I_X(\mathbf{x})$ as the indicator function such that $I_X(\mathbf{x}) = 1$ if $\mathbf{x} \in X$, and $I_X(\mathbf{x}) = 0$ otherwise. Let

$$U(\mathbf{p}, \epsilon(\mathbf{p}, t)) := \{\mathbf{x} \in \mathbb{R}^2 : \|\mathbf{x} - \mathbf{p}\| < \epsilon(\mathbf{p}, t)\}$$

be a circular neighborhood centered at \mathbf{p} , with radius $\epsilon(\mathbf{p}, t)$ specified as:

$$\epsilon(\mathbf{p}, t) := \epsilon_{\min} + (\epsilon'(\mathbf{p}, t) - \epsilon_{\min}) s\left(\sum_{i=1}^N I_{U(\mathbf{p}, \epsilon_{\min})}(\mathbf{p}_i)\right),$$

where $\epsilon'(\mathbf{p}, t)$ satisfies $\sum_{i=1}^N I_{U(\mathbf{p}, \epsilon'(\mathbf{p}, t))}(\mathbf{p}_i) = 1$, meaning that the circular neighborhood with radius $\epsilon'(\mathbf{p}, t)$ contains exactly one robot. The function $s(x) = \frac{2}{1+e^x}$ is a sigmoid function that smooths the variation of the neighborhood radius between ϵ_{\min} and $\epsilon'(\mathbf{p}, t)$. Note that $\epsilon'(\mathbf{p}, t)$ adapts to the positions of the robots, which causes $\epsilon(\mathbf{p}, t)$ to change over time. Thus, the adaptive selection of $\epsilon(\mathbf{p}, t)$ ensures that the neighborhood $U(\mathbf{p}, \epsilon(\mathbf{p}, t))$ always contains at least one robot.

Secondly, let $N_U := \sum_{i=1}^N I_{U(\mathbf{p}, \epsilon(\mathbf{p}, t))}(\mathbf{p}_i)$ denote the number of robots within $U(\mathbf{p}, \epsilon(\mathbf{p}, t))$. Let $S_U = \pi\epsilon(\mathbf{p}, t)^2$ denote its area. Then, the robot density at position \mathbf{p} can be approximated as:

$$\check{\rho}(\mathbf{p}, t) = \frac{N_U}{S_U}. \quad (5)$$

Remark 1: Note that ϵ_{\min} is chosen small enough to ensure precise *local* density approximation. In regions with sparse robot distribution, a large $\epsilon(\mathbf{p}, t)$ is required to ensure that U contains at least one robot. Although this reduces local precision, the approximation remains reliable. In such cases, the density is approximated by $\frac{1}{\pi\epsilon(\mathbf{p}, t)^2}$, where a larger $\epsilon(\mathbf{p}, t)$ yields a smaller $\check{\rho}(\mathbf{p}, t)$, consistent with the low density expected in sparse regions. This confirms that (5) accurately reflects the true local density, validating the robustness and reasonableness of the approximation. \square

The concept of local averaging can be traced back to kernel density estimation (KDE) [20], [25], which aims to construct a smooth probability density function from localized information. Here, we adaptively adjust the neighborhood size $\epsilon(\mathbf{p}, t)$, analogous to the bandwidth parameter in KDE, to control the smoothness of the local density approximation. This approach facilitates a smooth transition from discrete to continuous distributions, effectively mitigating the fluctuations caused by the discrete nature of robot positions. In brief, local averaging enables us to model the robot swarm as a continuous medium, thus we can propose the following assumption on continuity and differentiability for simplicity.

Assumption 3: Assume that $\check{\rho}(\mathbf{p}, t)$ is continuous with respect to \mathbf{p} and differentiable with respect to t .

Thirdly, let dA denote the area element. Based on Assumption 3, the total number of robots within the virtual tube \mathcal{T} can be approximated by $\int_{\mathcal{T}} \check{\rho}(\mathbf{p}, t) dA$. Based on this, we introduce a normalization factor $\mu = \frac{1}{\int_{\mathcal{T}} \check{\rho}(\mathbf{p}, t) dA}$ and provide the definition as follows.

Definition 3: For $(\mathbf{p}, t) \in \mathcal{T} \times [0, T]$, the *spatial density function* of robots within the virtual tube is defined as

$$\rho(\mathbf{p}, t) = \mu \check{\rho}(\mathbf{p}, t). \quad (6)$$

According to Definition 3, it follows that $\rho(\mathbf{p}, t) > 0$ and $\int_{\mathcal{T}} \rho(\mathbf{p}, t) dA = 1$ for $t \geq 0$.

Remark 2: The inclusion of μ enhances the model's scalability. As the number of robots $N \rightarrow \infty$, the spatial density function $\rho(\mathbf{p}, t)$ converges to a *probability density function*,

consistent with previous studies [20], [21]. In this framework, $\rho(\mathbf{p}, t)S_U$ represents the probability of finding a robot within the neighborhood U of position \mathbf{p} , thereby providing a probabilistic interpretation of swarm distribution. \square

Based on Assumption 3 and Definition 3, we proceed to develop the evolution model for a robot swarm. Consider any bounded subregion $D \subset \mathcal{T}$ as shown in Figure 5. The integral $\int_D \rho dA$ represents the *proportion* of robots within D . The rate of change of this proportion is given by $\frac{d}{dt} \int_D \rho dA = \int_D \frac{\partial \rho}{\partial t} dA$. According to the conservation law, this rate equals the inward flux across the boundary ∂D , i.e., $-\int_{\partial D} \rho \mathbf{v} \cdot \boldsymbol{\nu} ds$, where ds denotes the boundary element, \mathbf{v} is the velocity field in \mathcal{T} , and $\boldsymbol{\nu}$ is the outward unit normal on ∂D . By the divergence theorem, this flux can be rewritten as $-\int_D \nabla \cdot (\rho \mathbf{v}) dA$. Thus, we obtain $\int_D \frac{\partial \rho}{\partial t} dA = -\int_D \nabla \cdot (\rho \mathbf{v}) dA$. Since D is arbitrary, it follows that $\frac{\partial \rho}{\partial t} + \nabla \cdot (\rho \mathbf{v}) = 0$. Assume an initial density distribution $\rho_0(\mathbf{p})$ within \mathcal{T} . The no-flux boundary condition is imposed on $\partial \mathcal{T}$ as $\mathbf{n} \cdot (\rho \mathbf{v}) = 0$, where \mathbf{n} is the outward unit normal on $\partial \mathcal{T}$, ensuring robots move within \mathcal{T} without crossing the virtual tube boundary.

In summary, the evolution model of the spatial density function $\rho(\mathbf{p}, t)$ is formulated as follows:

$$\begin{aligned} \frac{\partial}{\partial t} \rho &= -\nabla \cdot (\rho \mathbf{v}), & (\mathbf{p}, t) \in \mathcal{T}_T; \\ \rho &= \rho_0, & (\mathbf{p}, t) \in \mathcal{T} \times \{0\}; \\ \mathbf{n} \cdot (\rho \mathbf{v}) &= 0, & (\mathbf{p}, t) \in S(\mathcal{T}_T). \end{aligned} \quad (7)$$

Despite the fact that the proposed model is primarily designed for scenarios involving a large number of robots ($N \gg 100$) [20], [21], it remains applicable to smaller swarms due to the incorporation of local averaging techniques. Additionally, by selecting large spatial scales (the area of the virtual tube \mathcal{T}) and long temporal scales (the duration of swarm movement), the macroscopic behavior of the swarm can be effectively captured, while short-term fluctuations arising from individual robots' discrete movements are smoothed out. These approaches ensure that the derived evolution model provides an accurate description of the swarm's collective dynamics, even when the number of robots is relatively small.

III. PROBLEM OVERVIEW AND FORMULATION

In addressing the problem of navigating robot swarms through virtual tubes, we observed that robots' spatial distribution plays a crucial role. Particularly, in narrow tubes with low flow capacity, uncontrolled robot distribution can easily lead to congestion, reducing traversal efficiency and increasing the risk of collisions, either between robots or with the tube boundaries. This has been demonstrated in Reference [16] and supported by the simulation results in Subsection V-B. Therefore, we aim to design and track a desired spatial density function that accounts for the flow capacity, thus to improve both efficiency and safety during the traversal.

To start with, let $\mathcal{S}_i(t) := \{\mathbf{x} \in \mathbb{R}^2 : \|\mathbf{x} - \mathbf{p}_i(t)\| \leq r_s\}$ be the i th robot's safety area. Suppose that at any given time t , the spatial distribution of the robot swarm within the virtual

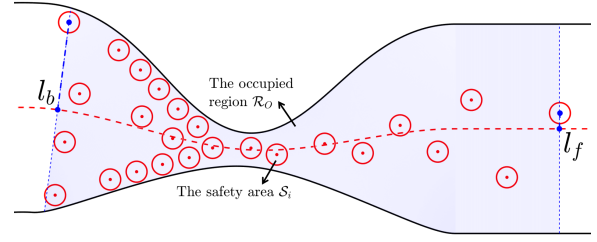


Fig. 6. Schematic diagram for the occupied region of the robot swarm.

tube is shown in Figure 6. The occupied region of the swarm is defined as

$$\mathcal{R}_O(t) := \cup_{l \in [l_b(t), l_f(t)]} \mathcal{C}(l), \quad (8)$$

where $l_b(t) = \min_{i=1, \dots, N} \{l_{\mathbf{p}_i(t)}\}$, $l_f(t) = \max_{i=1, \dots, N} \{l_{\mathbf{p}_i(t)}\}$, and $l_{\mathbf{p}_i(t)} = \omega(\mathbf{p}_i(t))$ from the mapping (2). For notational convenience, the time variable t is omitted henceforth.

Next, we design the desired spatial density function, denoted as ρ_d , which satisfies the following constraints. Firstly, by Definition 3, ρ_d should satisfy $\rho_d(\mathbf{p}, t) \geq 0, \forall \mathbf{p} \in \mathcal{T}$ and $\int_{\mathcal{T}} \rho_d(\mathbf{p}, t) dA = 1$. Secondly, assume that ρ_d is constant across the same cross-section, meaning that for any $\mathbf{p}' \in \mathcal{T}$, $\mathbf{p} \neq \mathbf{p}'$, if $l_{\mathbf{p}} = l_{\mathbf{p}'}$ then $\rho_d(\mathbf{p}, t) = \rho_d(\mathbf{p}', t)$. Additionally, we focus more on the spatial density within the swarm's occupied region \mathcal{R}_O , thus assume: $\rho_d(\mathbf{p}, t) \neq 0$ if $\mathbf{p} \in \mathcal{R}_O$, $\rho_d(\mathbf{p}, t) = 0$ otherwise. Lastly, for $\forall \mathbf{p} \in \mathcal{R}_O$, it is desired and reasonable to assume that $\rho_d(\mathbf{p}, t) = \lambda \sigma(l_{\mathbf{p}})$, where $\lambda > 0$, as cross-sections with greater flow capacity can accommodate more robots, corresponding to a higher robot density.

Based on the above analysis, the desired spatial density function ρ_d should satisfy the following necessary constraints:

$$\begin{cases} \rho_d(\mathbf{p}, t) = \lambda \sigma(l_{\mathbf{p}}), & \mathbf{p} \in \mathcal{R}_O; \\ \rho_d(\mathbf{p}, t) = 0, & \mathbf{p} \in \mathcal{T} \setminus \mathcal{R}_O; \\ \rho_d(\mathbf{p}, t) = \rho_d(\mathbf{p}', t), & l_{\mathbf{p}} = l_{\mathbf{p}'}; \\ \int_{\mathcal{T}} \rho_d(\mathbf{p}, t) dA = 1. \end{cases} \quad (9)$$

With these constraints, in the curvilinear coordinate system, it is straightforward to obtain that

$$\int_{l_b}^{l_f} \int_{-r_d(l)}^{r_u(l)} \lambda \sigma(l) dr dl = 1.$$

Solving for $\lambda = \frac{1}{\int_{l_b}^{l_f} 2r_c(l)^2 dl}$, hence ρ_d is designed as

$$\rho_d(\mathbf{p}, t) = \begin{cases} \frac{r_c(l_{\mathbf{p}})}{\int_{l_b}^{l_f} 2r_c(l)^2 dl}, & \mathbf{p} \in \mathcal{R}_O, \\ 0, & \mathbf{p} \in \mathcal{T} \setminus \mathcal{R}_O. \end{cases} \quad (10)$$

Summarizing the above overview, the problem studied in this article can be formulated as follows.

Problem 1: Design the saturated velocity command \mathbf{v}_i in (3) to meet the following three requirements.

- Navigate the robot swarm through the regular (possibly narrow) virtual tube. Specifically, for each \mathbf{p}_i , $i = 1, \dots, N$, there exists a corresponding time $t_i > 0$, such that $l_{\mathbf{p}_i(t_i)} = L$.

- Ensure that all robots avoid collisions both with each other and with the non-cross-sectional boundary of the virtual tube. Namely, $\mathcal{S}_i(t) \cap \mathcal{S}_j(t) = \emptyset$ and $\mathcal{S}_i(t) \cap \partial \mathcal{T}' = \emptyset$ for $t > 0$, $i, j = 1, \dots, N$, $i \neq j$.
- The global vector field \mathbf{v} corresponding to \mathbf{v}_i should drive the solution of (7) towards ρ_d , meaning that actual spatial density function (or distribution) of the robot swarm approaches the desired one.

IV. CONTROLLER DESIGN AND GUARANTEE OF SAFETY AND STABILITY

In this section, we firstly employ the modified artificial potential field method to ensure safe navigation of the robot swarm within the virtual tube. Secondly, we apply density feedback control to newly design a distribution regulation term for managing the robot swarm's configuration. Thirdly, by integrating the safe navigation term and the distribution regulation term, we design a novel and saturated controller, then obtain its corresponding global velocity field. Finally, under the global velocity field, we demonstrate that collision-free traversal through the virtual tube and tracking of the desired density can both be achieved, thus Problem 1 is solved.

A. Safe Navigation Design

In this subsection, we design control terms to enable safe navigation. In our previous work [22], we proposed a distributed controller for navigating robot swarm through a general virtual tube. This controller comprises three control terms: *Line Approaching*, *Robot Avoidance*, and *Virtual Tube Keeping*, which are derived from the associated Lyapunov-like functions.

Firstly, to ensure that the robot swarm approaches the terminal cross-section $\mathcal{C}(L)$, the Line Approaching term is designed and formulated as:

$$\mathbf{u}_{1,i} = \text{sat}((L - l_{\mathbf{p}_i})\eta(\mathbf{p}_i)\mathbf{t}_c(l_{\mathbf{p}_i}), k_1), \quad (11)$$

where k_1 is the maximum approaching speed, and the line integral Lyapunov function corresponding to the control term is set to be [22]:

$$V_{1,i} = \int_{\mathcal{V}_{\mathbf{p}_i}} \text{sat}(-(L - l_{\mathbf{x}})\eta(\mathbf{x}), k_1) dl_{\mathbf{x}},$$

where $dl_{\mathbf{x}}$ denotes the arc length element, $\mathcal{V}_{\mathbf{p}_i}$ represents the curve from \mathbf{p}_i to $\mathcal{C}(L)$ along the unit tangent vector $\mathbf{t}_c(\cdot)$, and $0 < \eta_{\min} \leq \eta(\mathbf{x}) \leq \eta_{\max}$ is the scaling factor.

Secondly, to prevent collisions between robots while constraining them within the virtual tube, the Robot Avoidance and Virtual Tube Keeping terms are respectively designed as

$$\begin{aligned} \mathbf{u}_{2,i} &= -k_2 \sum_{j \in \mathcal{N}_{m,i}} \frac{\partial V_{m,ij}}{\partial \|\tilde{\mathbf{p}}_{m,ij}\|} \frac{\tilde{\mathbf{p}}_{m,ij}}{\|\tilde{\mathbf{p}}_{m,ij}\|}, \\ \mathbf{u}_{3,i} &= -k_3 \frac{\partial V_{t,i}}{\partial \mathbf{p}_i}. \end{aligned} \quad (12)$$

Here, k_2 and k_3 are positive control gains, $\tilde{\mathbf{p}}_{m,ij} := \mathbf{p}_i - \mathbf{p}_j$ denotes the relative position between the i th and j th robots, and $\mathcal{N}_{m,i} := \{j : \|\tilde{\mathbf{p}}_{m,ij}\| \leq r_s + r_a\}$ denotes the set of

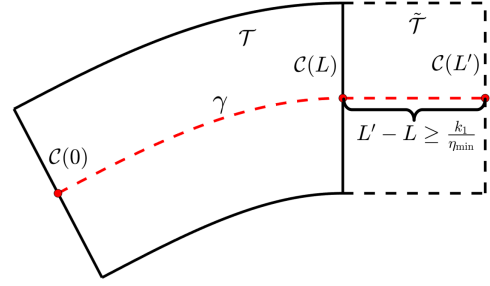


Fig. 7. The extend virtual tube $\tilde{\mathcal{T}}$ to modify $\mathbf{u}_{1,i}$

neighbors of the i th robot, where $r_a > r_s$ is the *avoidance radius* [22]. For the detailed information on $V_{m,ij}$ and $V_{t,i}$, please refer to [22]. This article primarily focuses on the distribution control of robot swarms within narrow virtual tubes; hence, the specifics of these three control terms are not further elaborated here.

Finally, by integrating the above three control terms, we design the *safe navigation* term as

$$\mathbf{u}_{123,i} = \mathbf{u}_{1,i} + \mathbf{u}_{2,i} + \mathbf{u}_{3,i}. \quad (13)$$

Remark 3: The Line Approaching term $\mathbf{u}_{1,i}$, defined in (11), is commonly used in stability analysis. However, for practical applications, we modify it as follows:

$$\mathbf{u}_{1,i} = \text{sat}((L' - l_{\mathbf{p}_i})\eta(\mathbf{p}_i)\mathbf{t}_c(l_{\mathbf{p}_i}), k_1) = k_1 \mathbf{t}_c(l_{\mathbf{p}_i}),$$

where $L' \geq L + k_1/\eta_{\min}$. This can be interpreted as extending the virtual tube \mathcal{T} along the generating curve γ and considering $\mathcal{C}(L')$ as the terminal cross-section, forming an extended virtual tube $\tilde{\mathcal{T}} = \cup_{l \in [0, L']} \mathcal{C}(l)$, as shown in Figure 7. In this case, the robot's Line Approaching term $\mathbf{u}_{1,i}$ within the original virtual tube \mathcal{T} maintains a constant magnitude, which simplifies the design and implementation of the control term. \square

B. Distribution Regulation Design

In this subsection, we introduce a newly designed distribution regulation term for the robot swarm to control its macroscopic configuration. While the safe navigation term (13) works effectively in general virtual tubes, its lack of distribution regulation in narrow virtual tubes can result in congestion, reduced traffic efficiency, and increased safety risks. Therefore, controlling the swarm's distribution within the tube is crucial.

The density evolution model (7) employs a partial differential equation (PDE) to describe the collective dynamics of the robot swarm, which establishes a connection between the dynamics of individual robots and their global behavior. The velocity field \mathbf{v} is expected to be designed such that ρ converges to ρ_d . Define the density tracking error $\Phi(\mathbf{p}, t) = \rho(\mathbf{p}, t) - \rho_d(\mathbf{p}, t)$, denote $\Phi_0(\mathbf{p}) = \rho_0(\mathbf{p}) - \rho_d(\mathbf{p}, 0)$. Substitute $\rho = \Phi + \rho_d$ into (7), then Φ satisfies

$$\begin{aligned} \frac{\partial}{\partial t}(\Phi + \rho_d) &= -\nabla \cdot ((\Phi + \rho_d)\mathbf{v}), \quad (\mathbf{p}, t) \in \mathcal{T}_T; \\ \Phi &= \Phi_0, \quad (\mathbf{p}, t) \in \mathcal{T} \times \{0\}; \\ \mathbf{n} \cdot ((\Phi + \rho_d)\mathbf{v}) &= 0, \quad (\mathbf{p}, t) \in S(\mathcal{T}_T). \end{aligned} \quad (14)$$

Our idea is to design \mathbf{v} such that Φ satisfies the following diffusion equation

$$\frac{\partial}{\partial t}\Phi(\mathbf{p}, t) - \alpha\Delta\Phi(\mathbf{p}, t) = 0, \quad (15)$$

where $\alpha > 0$ is the diffusion coefficient, Δ is the Laplacian operator. The solution to (15) will evolve toward a constant function of 0, because $\int_{\mathcal{T}}\Phi(\mathbf{p}, t)dA = \int_{\mathcal{T}}\rho(\mathbf{p}, t)dA - \int_{\mathcal{T}}\rho_d(\mathbf{p}, t)dA \equiv 1 - 1 = 0$ for any $t \geq 0$.

Assume that the density $\rho(\mathbf{p}, t)$ is strictly positive and can be accurately measured, then the global velocity field is designed as

$$\mathbf{v}(\mathbf{p}, t) = -\frac{\alpha(\nabla\Phi(\mathbf{p}, t) + \mathbf{w}_m(\mathbf{p}, t))}{\rho(\mathbf{p}, t)}, \quad (16)$$

where \mathbf{w}_m the correction term, satisfies $\|\mathbf{w}_m\|_{L^\infty(\mathcal{T}_T)} < \infty$, with the following constraints:

$$\begin{aligned} \nabla \cdot (\alpha\mathbf{w}_m(\mathbf{p}, t)) &= \frac{\partial\rho_d(\mathbf{p}, t)}{\partial t}, & (\mathbf{p}, t) \in \mathcal{T}_T; \\ \mathbf{n} \cdot \mathbf{w}_m(\mathbf{p}, t) &= 0, & (\mathbf{p}, t) \in S(\mathcal{T}_T). \end{aligned}$$

The asymptotic stability of system (14) under (16) is demonstrated in [26]. Furthermore, with the fact that $\int_{\mathcal{T}}\Phi dA \equiv 0$, we can apply the Poincaré inequality to obtain exponential stability [19].

However, in real practice, the calculation of $\rho(\mathbf{p}, t)$ is complex and challenging, therefore some reasonable estimations need to be taken. Kernel density estimation (KDE) is a nonparametric way to estimate an unknown density [25]. The common density $\rho(\mathbf{p}, t)$ can be estimated by N position samples $\{\mathbf{p}_i(t)\}_{i=1}^N$ and given by

$$\hat{\rho}(\mathbf{p}, t) = \frac{1}{Nh^2} \sum_{i=1}^N K\left(\frac{\mathbf{p} - \mathbf{p}_i(t)}{h}\right), \quad (17)$$

where h is the bandwidth, $K(\mathbf{x})$ is chosen as smooth Gaussian kernel function

$$K(\mathbf{x}) = \frac{1}{2\pi} \exp\left(-\frac{1}{2}\mathbf{x}^T\mathbf{x}\right).$$

With this estimation, we have $\lim_{N \rightarrow \infty} \|\hat{\rho}(\mathbf{p}, t) - \rho_d(\mathbf{p}, t)\|_{L^\infty(\mathcal{T})} = 0$ with probability 1 for $t \geq 0$. Therefore, the more robots there are in the swarm, the more accurate the density estimation becomes.

Using the density estimation (17), then the global velocity field (16) is modified to be

$$\mathbf{v}(\mathbf{p}, t) = -\frac{\alpha(\mathbf{p}, t)\nabla(\hat{\rho}(\mathbf{p}, t) - \rho_d(\mathbf{p}, t))}{\hat{\rho}(\mathbf{p}, t)}. \quad (18)$$

Here, we let α be the control gain that varies with space and time. Furthermore, we set $\mathbf{w}_m \equiv 0$ to simplify the controller design and implementation. The gradient of ρ_d can be computed as

$$\nabla\rho_d(\mathbf{p}, t) = \begin{cases} \frac{\frac{d}{dt}r_c(t)|_{t=\mathbf{p}}\nabla\omega(\mathbf{p})}{\int_{l_b}^{l_t} 2r_c(l)^2 dl}, & \mathbf{p} \in \mathcal{R}_O, \\ 0, & \mathbf{p} \in \mathcal{T} \setminus \mathcal{R}_O. \end{cases}$$

Subsequently, by applying (18) to the i th robot, we design the fourth control term, the *distribution regulation*, as

$$\mathbf{u}_{4,i}(\mathbf{p}_i, t) = -\frac{\alpha(\mathbf{p}_i, t)\nabla(\hat{\rho}(\mathbf{p}_i, t) - \rho_d(\mathbf{p}_i, t))}{\hat{\rho}(\mathbf{p}_i, t)}. \quad (19)$$

C. Controller Design

In this subsection, we integrate the safe navigation term (13) and the distribution regulation term (19), thus design a novel and saturated controller. Specifically, we let $\mathbf{u}_i := \mathbf{u}_{123,i} + \mathbf{u}_{4,i}$. Then the velocity command for (3) is designed as

$$\mathbf{v}_i = \text{sat}(\mathbf{u}_i, v_{\max}) = \kappa_m(\mathbf{u}_{123,i} + \mathbf{u}_{4,i}). \quad (20)$$

At this point, \mathbf{v}_i for the i th robot is in fact derived from the generalized global velocity field

$$\tilde{\mathbf{v}}(\mathbf{p}, t) = -\kappa_m \frac{\alpha(\mathbf{p}, t)\nabla(\hat{\rho}(\mathbf{p}, t) - \rho_d(\mathbf{p}, t)) - \hat{\rho}(\mathbf{p}, t)\mathbf{w}_e(\mathbf{p}, t)}{\hat{\rho}(\mathbf{p}, t)}, \quad (21)$$

where \mathbf{w}_e is regarded as an external vector field, satisfying

$$\mathbf{w}_e(\mathbf{p}_i, t) = \mathbf{u}_{123,i}. \quad (22)$$

Consequently \mathbf{v}_i can be considered as the result of $\tilde{\mathbf{v}}$ acting on \mathbf{p}_i .

Remark 4: Since N is finite, or equivalently, the position samples in (17) is limited, $\hat{\rho}(\mathbf{p}, t)$ is bounded in \mathcal{T}_T . Additionally, due to practical physical constraints, $\mathbf{u}_{123,i}$ is also bounded. Therefore, \mathbf{w}_e can be specifically chosen to satisfy $\|\hat{\rho}(\mathbf{p}, t)\mathbf{w}_e(\mathbf{p}, t)\|_{L^\infty(\mathcal{T})} < \infty$ and (22), which is helpful in the stability analysis of density tracking. \square

D. Guarantee of safety and stability

In this subsection, we present the main result of this article. Prior to this, some assumptions and useful lemmas are needed.

Assumption 4: Assume that for $i, j = 1, \dots, N$ and $j \neq i$, there exist $\mathcal{S}_i(0) \cap \mathcal{S}_j(0) = \emptyset$ and $\mathcal{S}_i(0) \cap \partial\mathcal{T} = \emptyset$. Namely all robots do not collide with each other and locate within the virtual tube at the initial moment.

Assumption 5: Once the i th robot reaches the terminal cross-section $\mathcal{C}(L)$, mathematically $l_{\mathbf{p}_i} = L$, it will immediately exit the virtual tube and no longer influence the motion of other robots.

Lemma 1 ([27]): Based on Assumptions 4 and 5, assume that the velocity command for the i th robot is (20). Then there exist sufficiently small ϵ_m and $\epsilon_s > 0$ in $\mathbf{u}_{2,i}$, and a sufficiently small $\epsilon_t > 0$ in $\mathbf{u}_{3,i}$, such that $\mathcal{S}_i(t) \cap \mathcal{S}_j(t) = \emptyset$ and $\mathcal{S}_i(t) \cap \partial\mathcal{T}' = \emptyset$ for all initial positions $\mathbf{p}_i(0)$, $t > 0$, $i, j = 1, \dots, N$, $i \neq j$.

Lemma 2 ([19]): Consider the evolution model (7), assume that $v_i \in L^\infty(\mathcal{T}_T)$, $\rho_0 \in L^\infty(\mathcal{T})$, and $\partial_i v_i \in L^\infty(\mathcal{T}_T)$. Suppose that $\rho_0 > 0$, then it follows that $\rho > 0$ for a.e. $t \in [0, T]$.

Lemma 3 ([19]): Consider the control system (14), and $\Phi \equiv 0$ is the equilibrium point. If (14) possesses a locally input-to-state (LISS) Lyapunov function, then it is LISS.

Now, we present the theorem related to *safe navigation* through the virtual tube and *tracking stability* of the desired spatial density function.

Theorem 1: For all robots modeled as (3), apply the controller (20) and assume that $\alpha(\mathbf{p}_i, t)$ in (19) satisfies

$$\max_{\mathbf{p}_i} (\|\mathbf{u}_{4,i}(\mathbf{p}_i, t)\| - \|\mathbf{u}_{123,i}(\mathbf{p}_i, t)\|) \leq 0. \quad (23)$$

Then it can be guaranteed that all robots will safely navigate through the virtual tube, with $\mathcal{S}_i(t) \cap \partial\mathcal{T}' = \emptyset$ and $\mathcal{S}_i(t) \cap$

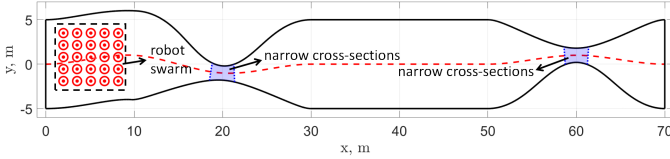


Fig. 8. The narrow regular virtual tube and initial distribution of the robots

$\mathcal{S}_j(t) = \emptyset$. Additionally, under the global velocity field $\tilde{\mathbf{v}}$ corresponding to (20), Φ in (14) is LISS if $\rho_0 > 0$ and

$$\left\| \frac{\nabla \varepsilon}{1 + \varepsilon} \right\|_{L^\infty(\mathcal{T})} < \frac{\alpha_{\min} \theta}{C \|\alpha\|_{L^\infty(\mathcal{T})}}, \quad (24)$$

where $\varepsilon(\mathbf{p}, t) := \hat{\rho}(\mathbf{p}, t)/\rho(\mathbf{p}, t) - 1$ is the estimation error, $C > 0$, $\theta \in (0, 1)$ are constants, and $\alpha_{\min}(t) := \inf_{\mathbf{p} \in \mathcal{T}} \alpha(\mathbf{p}, t) > 0$.

Proof: The theorem is proved in three steps. First, we show that robots neither collide with each other nor with the non-cross-sectional boundaries of the tube. Next, we demonstrate that under the controller (20), all robots reach the terminal cross-section $\mathcal{C}(L)$. Last, we prove that the density tracking error is LISS under the global velocity field (21). For a detailed proof, please refer to Appendix A. ■

Theorem 1 demonstrates that by incorporating the fourth distribution regulation term into the safe navigation term, the newly designed and saturated controller \mathbf{v}_i can still navigate the robot swarm through the virtual tube without collisions, provided that the added term $\mathbf{u}_{4,i}$ satisfies the constraint (23). Furthermore, the global vector field $\tilde{\mathbf{v}}$ corresponding to \mathbf{v}_i can render the density tracking error Φ to be LISS, meaning that Φ tends to be bounded in the L^2 sense, as long as the density estimation error ε satisfies (24). The boundedness of Φ indicates that the actual spatial density function ρ does not deviate significantly from the desired ρ_d , thus the robots will approximately achieve the desired distribution within the tube, thereby improving both traversal efficiency and safety. In summary, Theorem 1 shows that all requirements in Problem 1 can be met, hence the controller proposed in this article can effectively solve Problem 1.

V. SIMULATION RESULTS

A. Numerical Simulations

The effectiveness of the proposed method is verified in this subsection. Consider a narrow regular virtual tube as depicted in Figure 8. The kinematic model for all robots is given by (3). The centers of the red circles in the figure represent the current positions of the robots, with the radius indicating the safety radius r_s . An initial robot swarm composed of $N = 25$ robots is arranged in a square formation within the tube, with no collisions occurring among the robots. The settings for all parameters are provided in Table I. The arc length parameter intervals corresponding to the narrow cross-sections are [18.94, 21.61] and [59.09, 61.73], respectively, which are highlighted with light blue shading in the figure.

The screenshots from the simulation are depicted in Figure 9, which lasted for 30 seconds. The blue arrows represent the velocity of individual robots. Additionally, as illustrated

TABLE I
SIMULATION PARAMETER SETTINGS

k_1	k_2	k_3	r_s	r_a	h	$\varepsilon_m/\varepsilon_s/\varepsilon_t$	v_{\max}
2	1	1	0.5m	0.7m	2	10^{-6}	3m/s

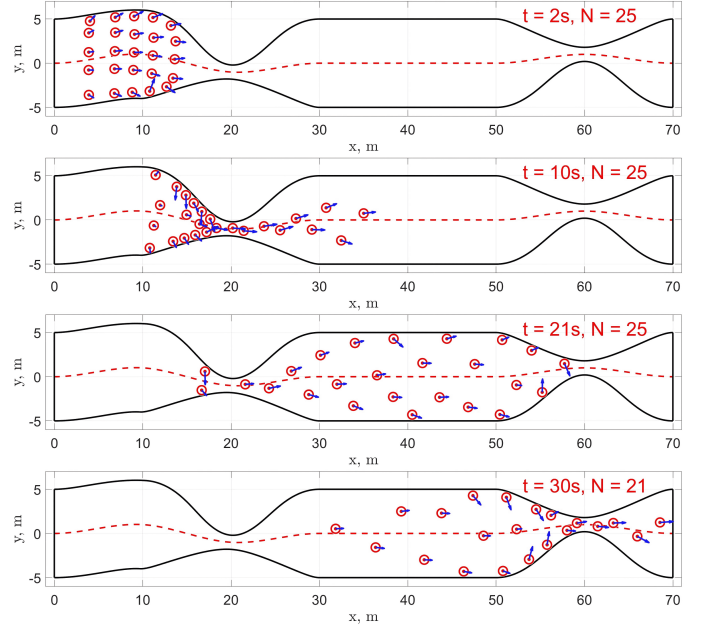


Fig. 9. Behavior of the robots under the controller \mathbf{v}_i

in Figure 10a and Figure 10b, the distance between any two robots is always greater than $2r_s = 1m$, and the minimum distance from $\partial\mathcal{T}'$ is always greater than $r_s = 0.5m$, implying that all robots can maintain their positions within the tube without colliding with each other.

Figure 11 demonstrates the error between the estimated density $\hat{\rho}(\mathbf{p}, t)$ and the robot swarm's desired density $\rho_d(\mathbf{p}, t)$ within \mathcal{R}_O . The convergence error, denoted as $\|\hat{\rho} - \rho_d\|_{L^2(\mathcal{R}_O)}$, is presented in Figure 12a. This shows that the error converges to a small neighborhood of 0 and remains bounded, which verifies the LISS of density tracking errors.

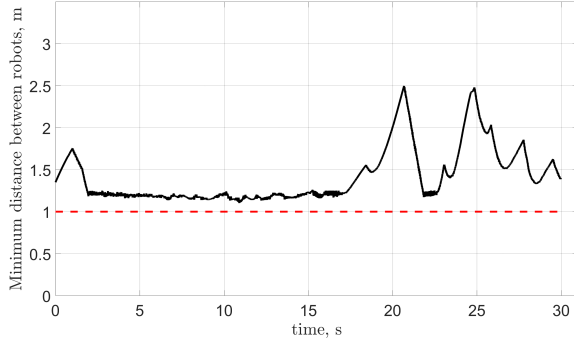
B. Simulation Comparisons

This subsection uses comparative simulations to highlight the advantages of incorporating the distribution regulation term into the controller in [22]. To characterize the degree of dispersion of the robot swarm within a virtual tube, we define the average minimum distance (*AMD*) as

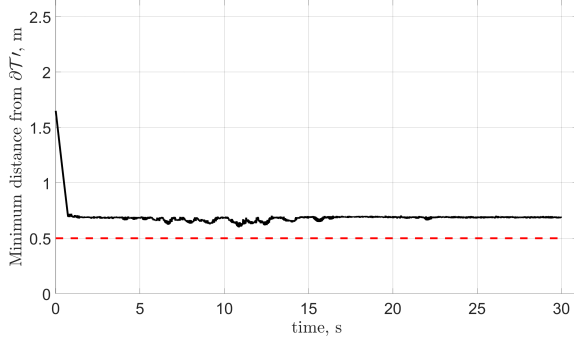
$$AMD = \frac{\sum_{i=1}^N \min_{j \in \{1, \dots, N\}, j \neq i} \|\tilde{\mathbf{p}}_{m,ij}\|}{N}. \quad (25)$$

Taking the highway traffic flow as an analogy: when the *AMD* is larger, the swarm is more dispersed, making it less likely for robots to form congestion while passing through narrow spaces. This results in improved traversal efficiency and safety.

If the distribution of the robot swarm is not controlled, i.e., when using only the controller $\mathbf{w}_i := \kappa_m \mathbf{u}_{123,i}$, the simulation screenshots are shown in Figure 13. Figure 14 compares the

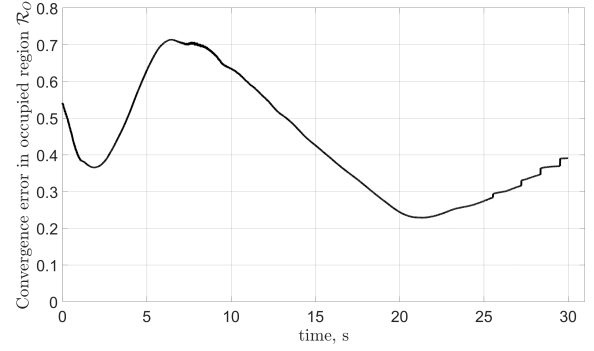


(a)

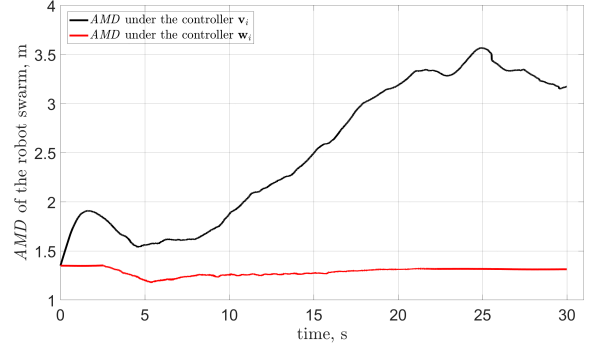


(b)

Fig. 10. (a) Minimum distance between robots. (b) Minimum distance from the tube boundary.



(a)



(b)

Fig. 12. (a) Evolution of the convergence error $\|\hat{\rho} - \rho_d\|_{L^2(\mathcal{R}_O)}$. (b) Evolution of AMD under controllers \mathbf{v}_i and \mathbf{w}_i .

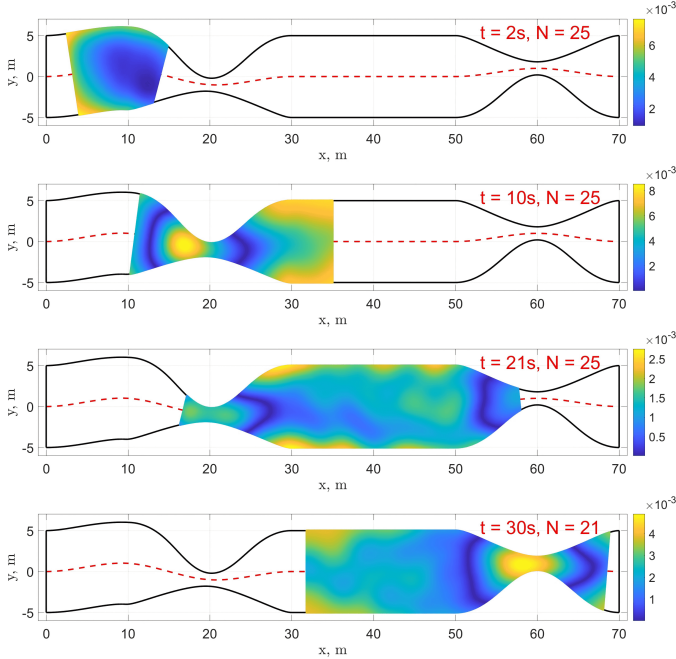


Fig. 11. Density error between $\hat{\rho}(\mathbf{p}, t)$ and $\rho_d(\mathbf{p}, t)$

trajectories of all robots under controllers \mathbf{v}_i and \mathbf{w}_i . It is clear that, during traversal, the robots maintain a compact formation. Even in sufficiently spacious regions, the robots do not disperse.

Figure 12b compares the AMD for controllers \mathbf{v}_i and \mathbf{w}_i .

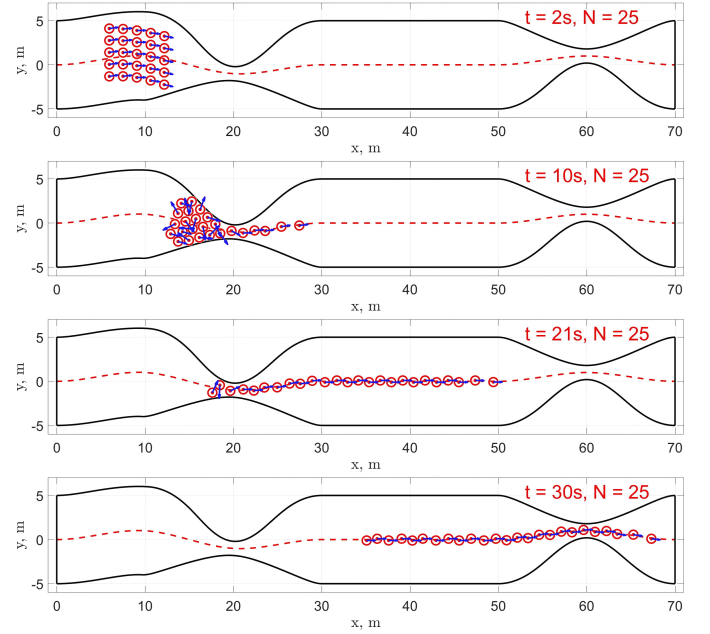


Fig. 13. Behavior of the robots under the controller \mathbf{w}_i

Additionally, by examining the simulation results at $t = 30$ s in Figures 9 and 13, we observe that four robots have already exited the tube under the controller \mathbf{v}_i , while no robots have exited under the controller \mathbf{w}_i . Based on the comparison of these simulation results, we conclude that utilizing the distribution regulation term effectively increases the AMD among

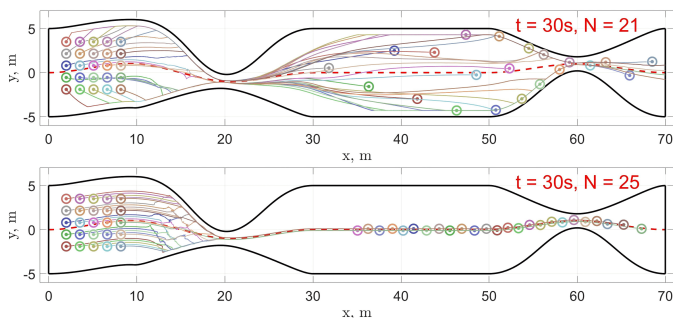


Fig. 14. Trajectories of all robots under controllers \mathbf{v}_i (top) and \mathbf{w}_i (bottom)

TABLE II
EXPERIMENT PARAMETER SETTINGS

k_1	k_2	k_3	r_s	r_a	h	$\varepsilon_m/\varepsilon_s/\varepsilon_t$	v_{\max}
0.05	1	1	$0.075m$	$0.12m$	0.15	10^{-6}	$0.1m/s$

robots. This leads to better dispersion, reduced congestion, and ultimately improves both efficiency and safety for the robot swarm during traversal through the virtual tube.

C. Realistic applications to ground mobile robots

In this subsection, we apply the proposed controller (20) to ground mobile robots, with the experiments conducted on the *Robotarium* platform [28], [29], developed by the Georgia Institute of Technology, which supports remote experimentation with multi-robot systems.

The parameters used in the experiment are provided in Table II. To demonstrate the applicability of our method to various virtual tubes, we consider robot swarm navigation in a regular annular virtual tube, as depicted in Figure 15. The minimum radius of the cross-section is $2r_s = 0.15m$, thus the annular virtual tube is narrow.

As shown in Figure 15, $N = 10$ robots stay within the tube and do not collide with each other at the initial moment. The experiment lasts for 150 seconds, the dashed lines in the figure represent the motion trajectories of the ground mobile robots. The experimental results show that the robots successfully avoid collisions and keep within the tube throughout the movement. Furthermore, as shown in Figures 16a and 16b, the distance between any two robots is always greater than $2r_s = 0.15m$, and the distance from each robot to the tube boundary remains greater than $r_s = 0.075m$. This further demonstrates safe and collision-free navigation within the annular virtual tube.

VI. CONCLUSION

This article addresses the challenge of spatial distribution, or macroscopic configuration control, for robot swarms navigating through narrow virtual tubes. We begin by originally defining the concepts of virtual tube area and flow capacity. Subsequently, a new density evolution model is developed, and a desired spatial density function is designed to derive the distribution regulation term. Next, a saturated velocity command is proposed by integrating this term with three

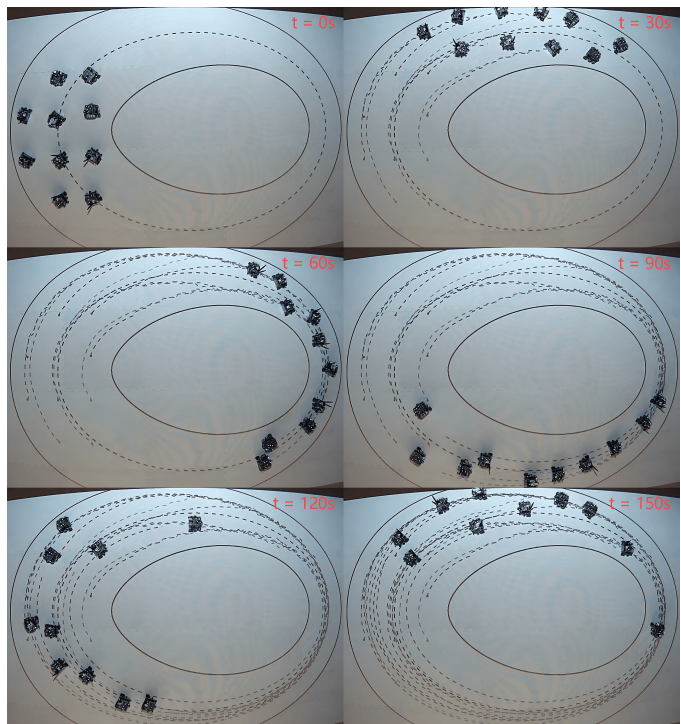
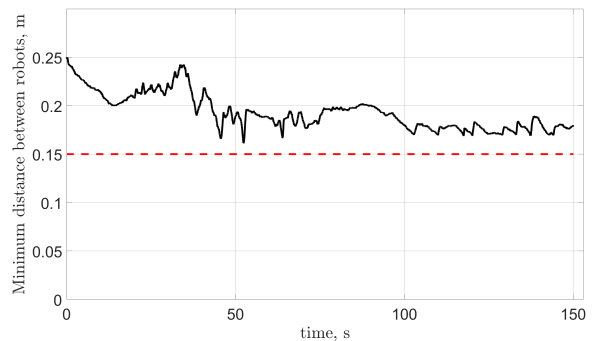
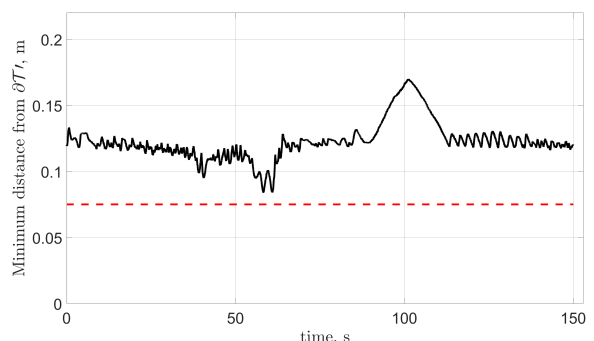


Fig. 15. Behavior of the ground mobile robots under the controller \mathbf{v}_i



(a)



(b)

Fig. 16. (a) Minimum distance between ground mobile robots. (b) Minimum distance from the tube boundary.

additional control terms, enabling collision-free navigation. The resulting global velocity field ensures the LISS of density tracking errors, allowing the swarm to maintain the desired distribution. This effectively improves the swarm's *AMD*, thus

enhances traversal efficiency and safety. Finally, simulation results and realistic applications validate our new approach's effectiveness and demonstrate its advantages in navigating robot swarms through narrow virtual tubes.

APPENDIX
PROOF OF THEOREM 1

(1) First, it follows from Lemma 1 that all robots will not collide with each other during the traversal, nor will they collide with the non-cross-sectional boundary of the tube.

(2) Next, consider the following Lyapunov-like function

$$V(t) = \sum_{i=1}^N \left(V_{1,i} + \frac{1}{2} \sum_{j=1, j \neq i}^N V_{m,ij} + V_{t,i} \right).$$

Then, differentiate V with respect to t and substitute (20), we obtain

$$\begin{aligned} \dot{V}(t) &= \sum_{i=1}^N \left(\text{sat}(-(L - l_{\mathbf{p}_i})\eta(\mathbf{p}_i)\mathbf{t}_c(l_{\mathbf{p}_i}), k_1) \right. \\ &\quad \left. + \sum_{j \in \mathcal{N}_{m,i}} \frac{\partial V_{m,ij}}{\partial \|\tilde{\mathbf{p}}_{m,ij}\|} \frac{\tilde{\mathbf{p}}_{m,ij}}{\|\tilde{\mathbf{p}}_{m,ij}\|} + \frac{\partial V_{t,i}}{\partial \mathbf{p}_i} \right) \cdot \mathbf{v}_i \\ &= \sum_{i=1}^N -\kappa_m \mathbf{u}_{123,i} \cdot (\mathbf{u}_{123,i} + \mathbf{u}_{4,i}) \\ &\leq \sum_{i=1}^N -\kappa_m \|\mathbf{u}_{123,i}\|^2 + \kappa_m \|\mathbf{u}_{123,i}\| \|\mathbf{u}_{4,i}\| \\ &\stackrel{(23)}{\leq} 0. \end{aligned}$$

Thus, similar to the proof of Theorem 1 in [22], we apply the invariant set principle to V , and conclude that $\mathbf{v}_i = 0$ is the unique equilibrium point. Furthermore, for the 1st robot with the maximum corresponding arc length parameter $l_{\mathbf{p}_1}$, from $\mathbf{v}_1 = 0$ it follows that $-(L - l_{\mathbf{p}_1})\eta(\mathbf{p}_1) \geq 0$, i.e., $l_{\mathbf{p}_1} \geq L$. Considering $l_{\mathbf{p}_1(0)} < L$ and the continuity of $l_{\mathbf{p}_1}$ over time, there exists $t_1 > 0$ such that $l_{\mathbf{p}_1(t_1)} = L$. By Assumption 5, once the 1st robot exits the virtual tube, we can apply the same analysis to the remaining robots. Thus, for each \mathbf{p}_i , $i = 1, \dots, N$, there exists a corresponding time $t_i > 0$ such that $l_{\mathbf{p}_i(t_i)} = L$. This implies that all robots will eventually reach the terminal cross-section $\mathcal{C}(L)$.

(3) Last, we prove the stability of the density tracking error Φ . Consider a candidate LISS Lyapunov function

$$\tilde{V}(t) = \frac{1}{2} \|\Phi\|_{L^2(\mathcal{T})}^2 = \frac{1}{2} \int_{\mathcal{T}} \Phi^2 dA. \quad (26)$$

Since ρ is a weak solution of (7), Φ is a weak solution of (14). According to [19], [30], there exists the following energy identity

$$\frac{1}{2} \int_{\mathcal{T}} \Phi^2 dA - \frac{1}{2} \int_{\mathcal{T}} \Phi_0^2 dA = \int_0^t \int_{\mathcal{T}} \nabla \Phi \cdot \mathbf{v}(\Phi + \rho_d) dA d\tau.$$

Then from (26),

$$\tilde{V}(t) - \tilde{V}(0) = \int_0^t \int_{\mathcal{T}} \nabla \Phi \cdot \mathbf{v}(\Phi + \rho_d) dA d\tau.$$

Hence, for a.e. $t \in [0, T]$,

$$\dot{\tilde{V}}(t) = \int_{\mathcal{T}} \nabla \Phi \cdot \mathbf{v}(\Phi + \rho_d) dA = \int_{\mathcal{T}} \nabla \Phi \cdot \mathbf{v} \rho_d dA. \quad (27)$$

From Lemma 2, $\rho > 0$, hence ε is well-defined. Rewrite $\rho = \Phi + \rho_d$ and $\hat{\rho} = \rho(1 + \varepsilon)$, then substitute (21) into (27). We have

$$\begin{aligned} \dot{\tilde{V}}(t) &= -\kappa_m \int_{\mathcal{T}} \nabla \Phi \cdot \left(\rho \frac{\alpha \nabla(\hat{\rho} - \rho_d) - \hat{\rho} \mathbf{w}_e}{\hat{\rho}} \right) dA \\ &= \kappa_m \int_{\mathcal{T}} -\nabla \Phi \cdot \frac{\alpha \nabla[\Phi(1 + \varepsilon)] + \alpha \nabla(\varepsilon \rho_d) - \hat{\rho} \mathbf{w}_e}{1 + \varepsilon} dA \\ &= \kappa_m \int_{\mathcal{T}} -\alpha |\nabla \Phi|^2 \\ &\quad - \nabla \Phi \cdot \frac{\alpha(\Phi + \rho_d) \nabla \varepsilon + \alpha \varepsilon \nabla \rho_d - \hat{\rho} \mathbf{w}_e}{1 + \varepsilon} dA \\ &\leq \kappa_m \int_{\mathcal{T}} -\alpha |\nabla \Phi|^2 + \left| \frac{\alpha \Phi \nabla \Phi \cdot \nabla \varepsilon}{1 + \varepsilon} \right| + \left| \frac{\alpha \rho_d \nabla \Phi \cdot \nabla \varepsilon}{1 + \varepsilon} \right| \\ &\quad + \left| \frac{\alpha \varepsilon \nabla \Phi \cdot \nabla \rho_d}{1 + \varepsilon} \right| + \left| \frac{\nabla \Phi \cdot \hat{\rho} \mathbf{w}_e}{1 + \varepsilon} \right| dA. \end{aligned} \quad (28)$$

Let $\alpha_{\min} := \inf_{\mathbf{p} \in \mathcal{T}} \alpha(\mathbf{p}, t) > 0$, then choose a constant $\theta \in (0, 1)$ to decompose $-\alpha |\nabla \Phi|^2$ into the following form

$$\begin{aligned} -\alpha |\nabla \Phi|^2 &= -\alpha(1 - \theta) |\nabla \Phi|^2 - \alpha \theta |\nabla \Phi|^2 \\ &\leq -\alpha_{\min}(1 - \theta) |\nabla \Phi|^2 - \alpha_{\min} \theta |\nabla \Phi|^2. \end{aligned} \quad (29)$$

Then apply the generalized Holder's inequality to the last four terms of the inequality in (28), apply the Poincaré inequality to the first and second terms of (29). Thus, there exists a constant $C > 0$ such that

$$\begin{aligned} \dot{\tilde{V}}(t) &\leq -\frac{\kappa_m \alpha_{\min}(1 - \theta)}{C^2} \|\Phi\|_{L^2(\mathcal{T})}^2 \\ &\quad - \frac{\kappa_m \alpha_{\min} \theta}{C} \|\nabla \Phi\|_{L^2(\mathcal{T})} \|\Phi\|_{L^2(\mathcal{T})} \\ &\quad + \kappa_m \|\alpha\|_{L^\infty(\mathcal{T})} \|\nabla \Phi\|_{L^2(\mathcal{T})} \|\Phi\|_{L^2(\mathcal{T})} \left\| \frac{\nabla \varepsilon}{1 + \varepsilon} \right\|_{L^\infty(\mathcal{T})} \\ &\quad + \kappa_m \|\alpha\|_{L^\infty(\mathcal{T})} \|\nabla \Phi\|_{L^2(\mathcal{T})} \|\rho_d\|_{L^2(\mathcal{T})} \left\| \frac{\nabla \varepsilon}{1 + \varepsilon} \right\|_{L^\infty(\mathcal{T})} \\ &\quad + \kappa_m \|\nabla \Phi\|_{L^2(\mathcal{T})} \|\alpha \nabla \rho_d\|_{L^\infty(\mathcal{T})} \left\| \frac{\varepsilon}{1 + \varepsilon} \right\|_{L^2(\mathcal{T})} \\ &\quad + \kappa_m \|\nabla \Phi\|_{L^2(\mathcal{T})} \|\hat{\rho} \mathbf{w}_e\|_{L^\infty(\mathcal{T})} \left\| \frac{1}{1 + \varepsilon} \right\|_{L^2(\mathcal{T})}. \end{aligned} \quad (30)$$

Thus we can now assert: If Φ satisfies

$$\begin{aligned} &\|\Phi\|_{L^2(\mathcal{T})} \\ &\geq \frac{\|\alpha\|_{L^\infty(\mathcal{T})} \|\rho_d\|_{L^2(\mathcal{T})} d(t) + \|\alpha \nabla \rho_d\|_{L^2(\mathcal{T})} d(t)}{\frac{\alpha_{\min} \theta}{C} - \|\alpha\|_{L^\infty(\mathcal{T})} d(t)} \\ &\quad + \frac{\|\hat{\rho} \mathbf{w}_e\|_{L^\infty(\mathcal{T})} d(t)}{\frac{\alpha_{\min} \theta}{C} - \|\alpha\|_{L^\infty(\mathcal{T})} d(t)} =: \chi(d(t)), \end{aligned} \quad (31)$$

then

$$\dot{\tilde{V}}(t) \leq -\frac{\kappa_m \alpha_{\min}(1 - \theta)}{C^2} \|\Phi\|_{L^2(\mathcal{T})}^2 =: -W \left(\|\Phi\|_{L^2(\mathcal{T})}^2 \right), \quad (32)$$

where

$$d(t) = \max\left\{\left\|\frac{\nabla\varepsilon}{1+\varepsilon}\right\|_{L^\infty(\mathcal{T})}(t), \left\|\frac{\varepsilon}{1+\varepsilon}\right\|_{L^2(\mathcal{T})}(t), \left\|\frac{1}{1+\varepsilon}\right\|_{L^2(\mathcal{T})}(t)\right\}.$$

Specifically, if (24) holds, with (31), then

$$\begin{aligned} \|\Phi\|_{L^2(\mathcal{T})} &\geq \frac{\|\alpha\|_{L^\infty(\mathcal{T})} \|\rho_d\|_{L^2(\mathcal{T})} \left\|\frac{\nabla\varepsilon}{1+\varepsilon}\right\|_{L^\infty(\mathcal{T})}}{\frac{\alpha_{\min}\theta}{C} - \|\alpha\|_{L^\infty(\mathcal{T})} \left\|\frac{\nabla\varepsilon}{1+\varepsilon}\right\|_{L^\infty(\mathcal{T})}} \\ &+ \frac{\|\alpha\nabla\rho_d\|_{L^\infty(\mathcal{T})} \left\|\frac{\varepsilon}{1+\varepsilon}\right\|_{L^2(\mathcal{T})}}{\frac{\alpha_{\min}\theta}{C} - \|\alpha\|_{L^\infty(\mathcal{T})} \left\|\frac{\nabla\varepsilon}{1+\varepsilon}\right\|_{L^\infty(\mathcal{T})}} \\ &+ \frac{\|\hat{\rho}\mathbf{w}_e\|_{L^\infty(\mathcal{T})} \left\|\frac{1}{1+\varepsilon}\right\|_{L^2(\mathcal{T})}}{\frac{\alpha_{\min}\theta}{C} - \|\alpha\|_{L^\infty(\mathcal{T})} \left\|\frac{\nabla\varepsilon}{1+\varepsilon}\right\|_{L^\infty(\mathcal{T})}}. \end{aligned} \quad (33)$$

Then the following inequality can be derived from (33).

$$\begin{aligned} \frac{\alpha_{\min}\theta}{C} \|\Phi\|_{L^2(\mathcal{T})} &\geq \|\alpha\|_{L^\infty(\mathcal{T})} \|\Phi\|_{L^2(\mathcal{T})} \left\|\frac{\nabla\varepsilon}{1+\varepsilon}\right\|_{L^\infty(\mathcal{T})} \\ &+ \|\alpha\|_{L^\infty(\mathcal{T})} \|\rho_d\|_{L^2(\mathcal{T})} \left\|\frac{\nabla\varepsilon}{1+\varepsilon}\right\|_{L^\infty(\mathcal{T})} \\ &+ \|\alpha\nabla\rho_d\|_{L^\infty(\mathcal{T})} \left\|\frac{\varepsilon}{1+\varepsilon}\right\|_{L^2(\mathcal{T})} \\ &+ \|\hat{\rho}\mathbf{w}_e\|_{L^\infty(\mathcal{T})} \left\|\frac{1}{1+\varepsilon}\right\|_{L^2(\mathcal{T})}. \end{aligned} \quad (34)$$

With (34), (32) can be obtained from (30), thus the assertion holds.

Furthermore, due to the fact that W in (32) is positive definite and χ in (31) belongs to

$$\mathcal{K} := \{f : \mathbb{R}_+ \rightarrow \mathbb{R}_+ \mid f \text{ is continuous and strictly increasing with } f(0) = 0\},$$

\tilde{V} is indeed an LISS Lyapunov function for (14). Thus by Lemma 3, Φ is LISS with respect to $d(t)$.

REFERENCES

- [1] S.-J. Chung, A. A. Paranjape, P. Dames, S. Shen, and V. Kumar, "A survey on aerial swarm robotics," *IEEE Trans. Robotics*, vol. 34, no. 4, pp. 837–855, Aug. 2018.
- [2] I. Navarro and F. Matía, "An introduction to swarm robotics," *Int. Scholarly Res. Notices*, vol. 2013, no. 1, pp. 608164, 2013.
- [3] K. Elamvazhuthi and S. Berman, "Mean-field models in swarm robotics: A survey," *Bioinspiration & Biomimetics*, vol. 15, no. 1, pp. 015001, 2019.
- [4] G. C. Maffettone, L. Liguori, E. Palermo, M. Di Bernardo, and M. Porfiri, "Mixed reality environment and high-dimensional continuification control for swarm robotics," *IEEE Trans. Control Syst. Technol.*, 2024.
- [5] P. Mao and Q. Quan, "Making robotics swarm flow more smoothly: a regular virtual tube model," in *Proc. IEEE/RSJ Int. Conf. Intelligent Robots and Systems (IROS)*, 2022, pp. 4498–4504.
- [6] P. Mao, R. Fu, and Q. Quan, "Optimal virtual tube planning and control for swarm robotics," *Int. J. Robotics Research*, vol. 43, no. 5, pp. 602–627, May 2024.
- [7] Y. Gao, C. Bai, and Q. Quan, "Distributed control for a multiagent system to pass through a connected quadrangle virtual tube," *IEEE Trans. Control Netw. Syst.*, vol. 10, no. 2, pp. 693–705, Apr. 2022.
- [8] Y. Gao, C. Bai, and Q. Quan, "Robust distributed control within a curve virtual tube for a robotic swarm under self-localization drift and precise relative navigation," *Int. J. Robust Nonlinear Control*, vol. 33, no. 16, pp. 9489–9513, Oct. 2023.
- [9] V. Crespi, A. Galstyan, and K. Lerman, "Top-down vs bottom-up methodologies in multi-agent system design," *Auton. Robots*, vol. 24, pp. 303–313, 2008.
- [10] Z. Sun, S. Mou, B. D. O. Anderson, and M. Cao, "Exponential stability for formation control systems with generalized controllers: A unified approach," *Syst. Control Lett.*, vol. 93, pp. 50–57, 2016.
- [11] J. Park, Y. Lee, I. Jang, and H. J. Kim, "Dlsc: Distributed multi-agent trajectory planning in maze-like dynamic environments using linear safe corridor," *IEEE Trans. Robotics*, vol. 39, no. 5, pp. 3739–3758, Oct. 2023.
- [12] R. T. Rodrigues, M. Basiri, A. P. Aguiar, and P. Mirdalo, "Low-level active visual navigation: Increasing robustness of vision-based localization using potential fields," *IEEE Robotics and Automation Letters*, vol. 3, no. 3, pp. 2079–2086, Jul. 2018.
- [13] A. M. C. Rezende, V. M. Goncalves, and L. C. A. Pimenta, "Constructive time-varying vector fields for robot navigation," *IEEE Trans. Robotics*, vol. 38, no. 2, pp. 852–867, Apr. 2021.
- [14] U. Borrmann, L. Wang, A. D. Ames, and M. Egerstedt, "Control barrier certificates for safe swarm behavior," *IFAC-PapersOnLine*, vol. 48, no. 27, pp. 68–73, 2015.
- [15] D. Sakai, H. Fukushima, and F. Matsuno, "Flocking for multirobots without distinguishing robots and obstacles," *IEEE Trans. Control Syst. Technol.*, vol. 25, no. 3, pp. 1019–1027, 2016.
- [16] W. Song, Y. Gao, and Q. Quan, "Speed and density planning for a speed-constrained robot swarm through a virtual tube," *IEEE Robotics and Automation Letters*, vol. 9, no. 11, pp. 10628–10635, Nov. 2024.
- [17] V. Deshmukh, K. Elamvazhuthi, S. Biswal, Z. Kakish, and S. Berman, "Mean-field stabilization of Markov chain models for robotic swarms: Computational approaches and experimental results," *IEEE Robotics and Automation Letters*, vol. 3, no. 3, pp. 1985–1992, Jul. 2018.
- [18] C. Sinigaglia, A. Manzoni, F. Braghin, and S. Berman, "Robust optimal density control of robotic swarms," *arXiv preprint arXiv:2205.12592*, 2022.
- [19] T. Zheng, Q. Han, and H. Lin, "Transporting robotic swarms via mean-field feedback control," *IEEE Trans. Automatic Control*, vol. 67, no. 8, pp. 4170–4177, Aug. 2021.
- [20] U. Eren and B. Açikmeşe, "Velocity field generation for density control of swarms using heat equation and smoothing kernels," *IFAC-PapersOnLine*, vol. 50, no. 1, pp. 9405–9411, 2017.
- [21] V. Krishnan and S. Martinez, "Distributed control for spatial self-organization of multi-agent swarms," *SIAM J. Control Optim.*, vol. 56, no. 5, pp. 3642–3667, 2018.
- [22] Q. Quan, Y. Gao, and C. Bai, "Distributed control for a robotic swarm to pass through a curve virtual tube," *Robotics and Autonomous Systems*, vol. 162, pp. 104368, 2023.
- [23] L. W. Tu, *An Introduction to Manifolds*, 2nd ed. New York, NY, USA: Springer, 2011, pp. 47–83.
- [24] A. J. Chorin and J. E. Marsden, *A Mathematical Introduction to Fluid Mechanics*, vol. 3. New York: Springer, 1990.
- [25] B. W. Silverman, *Density Estimation for Statistics and Data Analysis*, 2nd ed. London, U.K.: Routledge, 2018.
- [26] S. Lv, P. Mao, and Q. Quan, "Mean-field based time-optimal spatial iterative learning within a virtual tube," *IEEE Control Systems Letters*, vol. 8, pp. 2021–2026, 2024.
- [27] Q. Quan, R. Fu, M. Li, D. Wei, Y. Gao, and K.-Y. Cai, "Practical distributed control for VTOL UAVs to pass a virtual tube," *IEEE Trans. Intelligent Vehicles*, vol. 7, no. 2, pp. 342–353, Jun. 2022.
- [28] S. Wilson, P. Glotfelter, L. Wang, S. Mayya, G. Notomista, M. Mote, and M. Egerstedt, "The robotarium: Globally impactful opportunities, challenges, and lessons learned in remote-access, distributed control of multirobot systems," *IEEE Control Syst. Mag.*, vol. 40, no. 1, pp. 26–44, 2020.
- [29] D. Pickem, P. Glotfelter, L. Wang, M. Mote, A. Ames, E. Feron, and M. Egerstedt, "The robotarium: A remotely accessible swarm robotics research testbed," in *Proc. 2017 IEEE Int. Conf. Robotics Autom. (ICRA)*, 2017, pp. 1699–1706.
- [30] G. M. Lieberman, *Second Order Parabolic Differential Equations*, Singapore: World Scientific, 1996.